

# Molecular characterization of melanocyte stem cells in their niche

Masatake Osawa<sup>1,\*</sup>, Gyohei Egawa<sup>1</sup>, Siu-Shan Mak<sup>1</sup>, Mariko Moriyama<sup>1</sup>, Rasmus Freter<sup>1</sup>, Saori Yonetani<sup>1</sup>, Friedrich Beermann<sup>2</sup> and Shin-Ichi Nishikawa<sup>1</sup>

<sup>1</sup>Laboratory for Stem Cell Biology, RIKEN Center for Developmental Biology, 2-2-3 Minatojima Minami-machi, Kobe, Hyogo 650-0047, Japan

<sup>2</sup>Molecular Oncology, Swiss Institute for Experimental Cancer Research, National Center of Competence in Research, 1066 Epalinges, Switzerland

\*Author for correspondence (e-mail: mosawa@cdb.riken.jp)

Accepted 12 October 2005

Development 132, 5589–5599

Published by The Company of Biologists 2005

doi:10.1242/dev.02161

## Summary

Emerging evidence from stem cell (SC) research has strengthened the idea that SC fate is determined by a specialized environment, known as the SC niche. However, because of the difficulty of identifying individual stem cells and their surrounding components in situ, the exact mechanisms underlying SC regulation by the niche remain elusive. To overcome this difficulty, we employed melanocyte stem cells (MSCs), which allow the identification of individual SCs in the niche, the lower permanent portion of the hair follicle (HF). Here, we present molecular makers that can distinguish MSCs from other melanocyte (MC) subsets in the HF. We also describe a simple and robust method that allows gene expression profiling in individual SCs. After isolating individual MSCs

from transgenic mice in which the MCs are marked by green fluorescence protein (GFP), we performed single-cell transcript analysis to obtain the molecular signature of individual MSCs in the niche. The data suggest the existence of a mechanism that induces the downregulation of various key molecules for MC proliferation or differentiation in MSCs located in the niche. By integrating these data, we propose that the niche is an environment that insulates SCs from various activating stimuli and maintains them in a quiescent state.

Key words: Stem cells, Melanocytes, Gene expression profile, Stem cell niche, Hair follicle

## Introduction

Stem cells (SCs) are defined as cells that have a dual capacity to generate mature cells through differentiation and to maintain themselves through self-renewal. In a variety of adult regenerative tissues, such as blood, muscle, skin, and intestinal epithelium, SCs play a crucial role in the maintenance of tissue homeostasis by continuously replenishing the cells comprising the tissue throughout an organism's lifetime. Functionally, the SC system can be separated into three distinct compartments: SC, transient amplifying (TA) and terminally differentiated cell (DC) compartments (Potten and Loeffler, 1990). In contrast to the actively proliferating TA cells, the majority of SCs in a steady-state tissue are thought to be in a quiescent state, or in the G0/G1 phase of cell cycle, although SCs are capable of intensive proliferation when stimulated. These infrequently cycling SCs were commonly identified as long-term label-retaining cells (LRCs) through a 5-bromo-2-deoxyuridine (BrdU) nuclear-labeling experiment (Cotsarelis et al., 1990). For example, by using this labeling experiment, the replication rate of hematopoietic SCs (HSCs) was estimated to be once in 60 days in rodents, and once per year in non-human primates (Cheshier et al., 1999; Mahmud et al., 2001). Why and how the relative quiescence of SCs is maintained is one of the central questions of SC biology. Recent loss-of-function studies demonstrate that the proliferation of certain types of SC is negatively regulated by several cell-cycle inhibitors, such as

p21<sup>cip/waf1</sup>, p27<sup>kpl</sup> and Pten (Cheng et al., 2000; Groszer et al., 2001; Walkley et al., 2005). In fact, in p21<sup>cip/waf1</sup> mutant mice, the proliferation of HSCs and neural SCs (NSCs) is dramatically increased, which consequently leads to SC exhaustion (Cheng et al., 2000; Groszer et al., 2001). Thus, the relative quiescence of SCs is crucial for maintaining the size of the SC compartment and for regulating the longevity of SCs; however, the exact molecular mechanisms underlying the regulation of the quiescent status of SCs are still largely unknown.

It is widely accepted that SCs are maintained by a specialized microenvironment known as the SC niche (Fuchs et al., 2004; Schofield, 1978; Spradling et al., 2001; Watt and Hogan, 2000). Although recently the importance of the niche in regulating SCs has been clarified intensively, the niche itself has remained a hypothetical entity for many SC systems, especially in vertebrates. This is in clear contrast to germline SCs (GSCs) in the *Drosophila* ovary or testis, where the nature of the cells comprising the niche and their role in the maintenance of GSCs have been well characterized, at both the cellular and the molecular level (Kiger et al., 2001; Spradling et al., 2001; Tulina and Matunis, 2001; Xie and Spradling, 2000). One clear difference between the *Drosophila* GSC system from those of vertebrates is the ability to identify individual SCs and the cells comprising the niche by their location and morphology. These features of *Drosophila* GSCs

offer experimental advantages in understanding the exact molecular interactions between the SCs and the niche. By contrast, in vertebrates, it is often the case that the SC compartment consists of extremely rare populations of cells, and that the microenvironment surrounding the SCs has a complicated anatomical structure that is occupied by many of the SC progeny in the TA/DC compartment. It is therefore difficult to identify the exact location of individual SCs and their niche, and to determine whether the surrounding SC progeny or different cell types are involved in the niche. These difficulties in the vertebrate SC systems hamper the detailed analysis of SC regulation by the niche.

Melanocytes (MCs) provide an attractive model with which to understand the molecular basis of various cellular regulations, as dysfunction of the molecules implicated in MC regulation (i.e. in survival, proliferation, migration or differentiation) can be easily identified by the coat color defect. Such understanding also provides a cue to define the molecular mechanism of SC regulation, as it has been reported recently that improper maintenance of MSCs causes hair to turn gray (Nishimura et al., 2005). Indeed, more than 90 different loci have currently been identified as coat color mutants in the mouse (Nakamura et al., 2002). Among these loci, *Pax3*, *Sox10*, *Mitf*, *Kit* (previously known as *c-Kit*) and *Ednrb* have been shown to be particularly critical for the development of immature MCs, melanoblasts (Mbs) (Goding, 2000; Nishikawa et al., 1991; Potterf et al., 2001; Shin et al., 1999).

Mbs emerge in the neural crest and migrate through the epidermis towards newly developing hair follicles (HFs) until all the Mbs in the hairy skin region become specifically localized in the HF. Once localized in the HF, they are separated into two populations: differentiated MCs, which are localized in the hair matrix region and are responsible for hair pigmentation; and MSCs, which are localized at the lower permanent portion of the HF and are responsible for the repopulation of the MC system in subsequent hair cycles. Previously, we demonstrated that MSCs are identified as the LRCs, and that they can survive even after blocking Kit signaling with a specific antagonistic antibody against Kit, which is normally essential for the proliferation and survival of all other subsets of MCs (Nishimura et al., 2002). However, except for this phenomenon, little is known about MSCs.

MSCs exemplify one SC system in which the SC compartment is anatomically segregated from the SC progeny in the TA/DC compartment (Nishimura et al., 2002). For these SCs, the cells comprising the niche, if they exist, should not be of the MC lineage because MSCs are scattered in the lower permanent portion of the HF without forming into cell clusters. This simple architecture of MSCs is expected to be advantageous for the investigation of molecular interactions between SCs and the niche, as has been learnt from examples of GSCs in *Drosophila*. The ultimate goal of our studies on MSCs is to define the exact molecular mechanisms of SC regulation in the niche. To achieve this goal, it is important to characterize the MSCs and to isolate them specifically, which would thus enable us to obtain a series of gene expression profiles of MSCs in the niche. Here, we describe (1) the molecular markers distinguishing MSCs from other cells, (2) the isolation of single MSCs from transgenic mice with MCs marked by GFP, and (3) the gene expression profiling of

individual MSCs using a single-cell cDNA amplification technique.

## Materials and methods

### Mice

*CAG-CAT-EGFP* mice (C57BL/6, a gift from Dr J. Miyazaki, Osaka University, Japan) were bred with *Dct<sup>tm1(Cre)Bee</sup>* mice (Guyonneau et al., 2004) to generate compound heterozygotes. Genotyping was performed as described previously (Guyonneau et al., 2004). *Dct-lacZ* mice (ICR, a gift from Dr I. Jackson, MRC Western General Hospital, UK) were maintained in our animal facility, as described previously (Nishimura et al., 2002). All animal experiments were performed in accordance with the guidelines of the RIKEN Center for Developmental Biology for animal and recombinant DNA experiments.

### Immunohistochemistry and in situ hybridization

To analyze the molecular markers for MSCs, immunofluorescent staining was performed using dorsal skin sections prepared from postnatal day 6 (P6) *Dct-lacZ* mice that were pre-treated with the anti-c-Kit antibody (Ack2) at P0, P2 and P4, as described previously (Nishimura et al., 2002). For the immunohistochemical analysis of TA cells/DCs in the hair matrix, non-treated P6 skin samples were used. Frozen skin sections were prepared as described previously (Nishimura et al., 2002). After treatment with a blocking solution containing 5% skim milk (Difco), 1% donkey serum (Chemicon) and 0.1% Triton X-100 (Nakarai-Tesque, Japan) in PBS, skin sections were incubated with primary antibodies diluted in the blocking solution. The following primary antibodies were used in the analysis: rabbit-anti- $\beta$ -gal (Chemicon), goat-anti- $\beta$ -gal (Biogenesis, UK), rabbit-anti-Dct, rabbit-anti-Tyrp1, rabbit-anti-Si (pMel17) (gifts from Dr V. Hearing, NIH, USA), goat-anti-Dct, goat-anti-Tyrosinase (Santa Cruz), mouse-anti-Lef1 (Upstate), mouse anti-Sox10 (a gift from Dr M. Wegner, University of Erlangen-Nurnberg, Germany), rabbit-anti-Sox10 (Chemicon), rabbit-anti-Pax3 (a gift from Dr G. Grosveld, St. Jude Children's Research Hospital, USA), rat-anti-c-Kit (Ack4, prepared in our laboratory) and rabbit-anti-Mitf (a gift from Dr H. Yamamoto, Tohoku University, Japan). The sections were then washed three times in PBS containing 0.1% Triton X-100, and incubated with an appropriate combination of the following secondary antibodies diluted in blocking solution containing TO-PRO3 (Molecular Probes): Alexa488-conjugated donkey anti-rabbit IgG, Alexa488-conjugated donkey anti-goat IgG, Alexa546-conjugated donkey anti-rabbit IgG, Alexa546-conjugated donkey anti-goat IgG (Molecular Probes) and Alexa488-conjugated donkey anti-mouse IgG (Jackson Laboratory). After washing three times with PBS, the slides were mounted with a ProLong Antifade kit (Molecular Probes) and observed under a confocal microscope (Bio-Rad Radiance 2100 or Zeiss LSM510 Meta).

For in situ hybridization/immunohistochemical double staining, in situ hybridization was performed as described previously (Wilkinson and Nieto, 1993), with a digoxigenin-labeled antisense probe using skin sections from *Dct-lacZ* mice. A *Sox10* antisense probe was synthesized from rat *Sox10* cDNA (a gift from Dr M. Wegner, University of Erlangen-Nurnberg, Germany). The *Sox10* probe was detected with goat peroxidase-conjugated anti-digoxigenin antibody (Roche) using the TSA plus Fluorescein system (Perkin Elmer Life Sciences), according to the manufacturer's protocol. After in situ hybridization, the sections were incubated with diluted rabbit anti- $\beta$ -gal antibody (Chemicon), washed three times in PBS and then incubated with donkey Alexa 546-conjugated anti-Rabbit IgG (Molecular Probes) to visualize *lacZ*<sup>+</sup> MCs.

### Isolation of single MCs

Dorsal skin was isolated from P6 *CAG-CAT-EGFP*; *Dct<sup>tm1(Cre)Bee</sup>* mice

## Development and disease

that were either pre-treated or not treated with Ack2. Embryonic skin (E16.5) was incubated in PBS containing 5 mM EDTA for 1 hour at 37°C and then the dermis was removed from the epidermis under stereomicroscopy. The embryonic epidermis was further dissociated by treatment with 0.25% Trypsin and 1 mM EDTA in PBS for 5 minutes at 37°C to obtain a single-cell suspension. Dorsal skin was incubated with 1 mg/ml collagenase type VI (Gibco) for 1 hour at 37°C and then the dermis was removed. Single HF s were isolated from the epidermis and micro-dissected to separate the lower permanent portion and the hair matrix regions. The lower permanent portion and hair matrix were then dissociated into single cells by treatment with 0.05% trypsin and 1 mM EDTA for 5 minutes at 37°C. Following neutralization with ice-cold PBS containing 20% FCS and 1 mM CaCl<sub>2</sub>, single GFP<sup>+</sup> MCs were individually picked with capillary pipettes.

### Single-cell PCR

Single cells were seeded separately into PCR tubes with 4.5 µl lysis buffer containing 50 mM Tris-HCl, 75 mM KCl, 5 units Super RNaseIN (Ambion), 7.5 units PrimeRNase Inhibitor (Eppendorf), 0.5% NP40, 1 mM DTT, 50 µM dNTP, and 15 nM MO-dT30 primer (AAGCAGTGGTATCAACGCAGAGTGGCCATTACGCCGTAC-TT-(dT)<sub>30</sub>). Tubes were then incubated at 65°C for 5 minutes and cooled to 45°C for 2 minutes. Reverse transcription was then carried out by the addition of 25 units of *Reverse-iT* Blend (AB Gene). After incubation at 50°C for 5 minutes, the reaction was terminated by heating at 70°C for 10 minutes. Next, 5 µl of reaction mixture [1×PCR buffer (Invitrogen), 1.5 mM MgCl<sub>2</sub>, 3 mM dATP, 15 units TdT (Promega) and 2 units RNaseH (Invitrogen)] was added into each tube and poly (A) tailing and RNA digestion performed by incubating at 37°C for 15 minutes, and then inactivating at 70°C for 10 minutes. cDNA amplification was carried out using HS ExTaq polymerase (Takara Biochemicals, Japan). Briefly, polyA-tailed cDNA (10 µl) was split into two tubes containing 45 µl of primary PCR reaction solution containing ExTaq PCR buffer (Takara Biochemicals), 5 mM MgCl<sub>2</sub>, 2 mM dNTP, 2 µM MO-dT30 primer and 5 units of HS ExTaq polymerase (Takara Biochemicals). PCR was performed with one cycle of 1 minute at 94°C, 2 minutes at 50°C and 2 minutes at 68°C, followed by 24 cycles of 30 seconds at 94°C, 30 seconds at 65°C, and 2 minutes at 72°C. After combining split tubes into one tube, cDNA was purified with Qiagen PCR purification kit according to manufacturer's procedure.

### Real-time PCR analysis

Real-time PCR analysis was carried out using a Qiagen QuantiTect SYBR Green PCR Kit according to the manufacturer's protocol. Briefly, cDNA was added to 14 µl of real-time PCR mix containing 2×QuantiTect SYBR green master mix and 0.3 µM each of specific primer pairs. PCR was performed at 95°C for 15 minutes for the initial activation of HotStarTaq polymerase, then with 40 cycles of 20 seconds at 95°C and 1 minute at 60°C using a ABI PRISM 7900 HT sequence detection system. Information on the PCR primer sets used in this study is available upon request. To test the fidelity of our cDNA amplification, we estimated the relative gene expression levels of individual genes in the amplified cDNA and examined how these correlated with the corresponding values obtained with unamplified cDNA. For this purpose, total RNA was extracted from a Mb cell line, Melb-a (a gift from Dr D. Bennett, St. George's Hospital, UK) (Sviderskaya et al., 1995), using Isogen (Nippon Gene, Japan) according to the manufacturer's protocol. To generate unamplified cDNA, 100 ng of total RNA was reverse transcribed with 5 µM (dT)<sub>20</sub> primer (Invitrogen) with 25 units of *Reverse-iT* Blend (AB Gene) containing 5× first strand buffer (Invitrogen), 5 mM DTT, 0.5 mM dNTP and 40 units RNaseOUT (Invitrogen), and then incubated at 45°C for 60 minutes and treated with 2 units of RNaseH at 37°C for 15 minutes. The unamplified cDNA was purified with a Qiagen PCR purification Kit and 1 ng of cDNA was used for real-time PCR

## Molecular characterization of melanocyte stem cells 5591

analysis as described above. To generate amplified cDNA, 10 pg of total RNA was used for the cDNA amplification as described above. Relative expression values were calculated by dividing the expression value of each target gene by that of a mRNA spike as described below.

### Spiking experiments

Poly(A)-tailed *Arabidopsis thaliana* LTP4 (GenBank Accession number AF159801), LTP6 (GenBank Accession number AF159803), NAC1 (GenBank Accession number AF198054) and TIM (GenBank Accession number AF247559) RNA was purchased from Stratagene and added into the lysis buffer containing either a single cell or 10 pg of total RNA prepared from the cultured melanoblast cell line Melb-a, to the following final concentrations: LTP4, 10<sup>-1</sup> pg/sample; LTP6, 10<sup>-2</sup> pg/sample; NAC1, 10<sup>-3</sup> pg/sample; TIM, 10<sup>-4</sup> pg/sample. Assuming 1 µg of RNA with an average length of ~500 bp is equal to 6 pmol, these concentrations correspond to 4×10<sup>4</sup>, 4×10<sup>3</sup>, 4×10<sup>2</sup> and 40 copies/sample, respectively. Each sample was reverse transcribed and amplified as described. Relative expression value was determined by Q-PCR using a primer pair specific for each spike RNA. For the normalization of each spike RNA and the melanogenic gene, LTP4 was used as a standard.

## Results

### Molecular markers distinguishing MSCs from the other compartments

First, we tried to determine the molecular markers that could distinguish MSCs from the TA/DC compartments. For this purpose, we used transgenic mice carrying the *lacZ* reporter gene under the control of the MC-specific *Dct* promoter to identify MCs with high sensitivity (Jordan and Jackson, 2000; Mackenzie et al., 1997). We have previously demonstrated that, by treating neonatal mice with Ack2, MSCs are identifiable at the lower permanent portion region of the guard hairs, whereas all other subsets of MCs were eliminated from the HF (Nishimura et al., 2002). HF morphogenesis in the postnatal skin is substantially unsynchronized, with spontaneous development of several different types of hair. In order to standardize our experiments, we regarded these Ack2-resistant MCs localized at the lower permanent portion of the guard hairs at stage 8 of HF morphogenesis (Paus et al., 1999) as MSCs, as it has been previously shown that dormant MSCs appear from this stage (Nishimura et al., 2005).

To compare the molecular expression profile of MSCs with that of TA/DC subsets of MCs localized at the hair matrix region, we prepared skin sections either from the Ack2-treated or the control mice and analyzed the expression of *Dct*, *Tyr*, *Si*, *Tyrp1*, *Kit*, *Pax3*, *Mitf*, *Sox10* and *Lef1* in these MC subsets by multicolor immunohistochemical staining. Consistent with our previous studies, and with those of other groups (Botchkareva et al., 2001; Nishimura et al., 2002), β-galactosidase<sup>+</sup> (β-gal<sup>+</sup>) MCs localized either at the lower permanent portion of the HF in the Ack2-treated skin or in the hair matrix region of the HF in the control skin. However, expression of *Tyr*, *Si*, *Tyrp1*, *Kit*, *Mitf*, *Sox10* and *Lef1* was undetectable in MSCs, whereas all of these molecules were expressed in the MCs at the hair matrix region (Fig. 1). Contrastingly, expression of *Dct* and *Pax3* was observed in MCs in both populations (Fig. 1). *Mki67* was undetectable in MSCs, whereas some TA subsets in the hair matrix were positive for *Mki67* (Fig. 1), indicating that MSCs are resting, whereas certain populations of the matrix MCs are actively proliferating. Thus, the MSC and TA/DC subsets were clearly

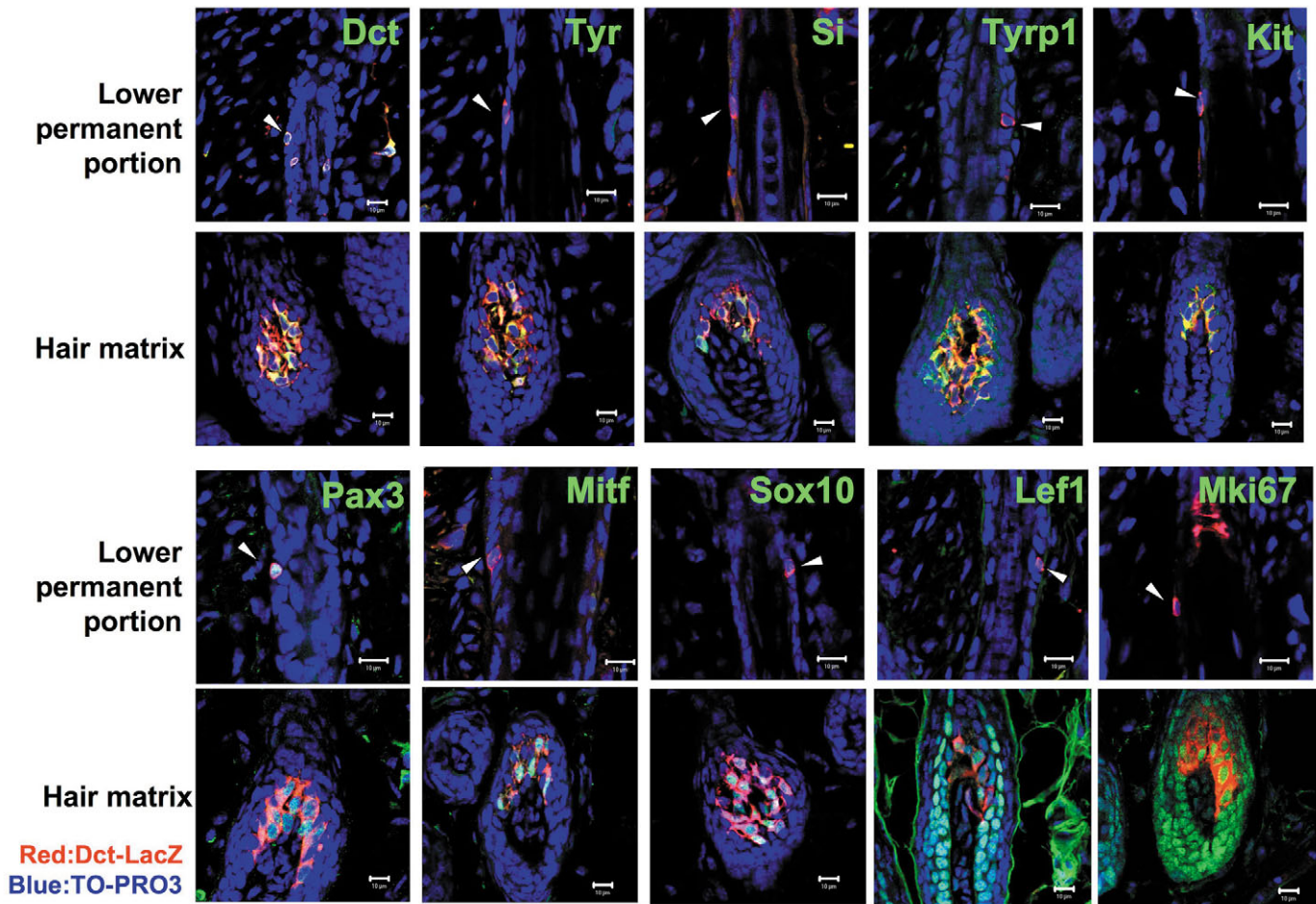


**Fig. 1.** Immunohistochemical characterization of the MSCs. Phenotypical characterization of MSCs in the lower permanent portion of the hair follicle (top) and MCs in the hair matrix region (bottom) in stage 8 guard hairs. Skin sections were stained with antibodies against *Dct*, *Tyr*, *Si*, *Tyrp1*, *Kit*, *Pax3*, *Mitf*, *Sox10*, *Lef1* or *Mki67* (green), and with anti- $\beta$ -gal (red). Nuclear staining (blue) was with TO-PRO3. Arrowheads indicate MSCs in the lower permanent portion of the hair follicle. Scale bars: 10  $\mu$ m.

distinguishable by their molecular expression patterns; the MSC subset being *Dct*<sup>+</sup>, *Pax3*<sup>+</sup>, *Tyr*<sup>-</sup>, *Si*<sup>-</sup>, *Tyrp1*<sup>-</sup>, *Kit*<sup>-</sup>, *Mitf*<sup>-</sup>, *Sox10*<sup>-</sup>, *Lef1*<sup>-</sup> and *Mki67*<sup>-</sup>, while, in contrast, the TA/DC subset was positive for all these markers.

It has been shown that *Sox10* plays a crucial role in the proper development of MCs (Mollaaghababa and Pavan, 2003). *Sox10* acts synergistically with *Pax3* in activating the transcription of *Mitf*, which, in turn, acts as a master regulator and controls the proliferation, differentiation and survival of MCs by controlling the expression of various melanogenic genes, such as *Dct*, *Tyrp1* and *Tyr* (Bondurand et al., 2000; Goding, 2000; McGill et al., 2002; Mollaaghababa and Pavan, 2003; Potterf et al., 2001). Indeed, as shown in Fig. 1 and Fig. 2A,B, *Sox10* was expressed in almost all of the MCs in the hair matrix and the Mbs in E16.5 and E18.5 embryos. Interestingly, at postnatal day 2 (P2), downregulation of *Sox10* was evident in Mbs colonized at the lower permanent portion of the HF (Fig. 2C,D). At P4, approximately 60% of  $\beta$ -gal<sup>+</sup> Mbs at this region became downregulated for *Sox10*, although its expression was detectable in almost all of the matrix MCs (Fig. 2D). To examine whether the downregulation of *Sox10* protein in the Mbs was accompanied by the downregulation of

its transcript, we performed in situ hybridization to detect *Sox10* mRNA expression in these Mbs. Consistent with *Sox10* protein expression in Mbs, *Sox10* mRNA was also detectable in Mbs in the developing HF (Fig. 2E). By contrast, its downregulation was evident in the Mbs that colonized in the lower permanent portion of the HF, whereas the intensive *Sox10* expression was maintained in MCs in the hair matrix (Fig. 2F).

From these observations, *Sox10* expression was shown to delimit the boundary between MSCs and other subsets of MCs in the HF. Thus, it is clear that MSCs display a distinct molecular expression profile from that of epidermal Mbs or the MCs at the hair matrix, which suggests the existence of discrete molecular expression programs among these populations.

### Isolation of MSCs from single HFs

These molecular expression analyses raised the possibility that MSCs could be further defined by their own gene expression profile, in addition to their biological properties (i.e. resistance against Ack2 treatment and specific localization at the lower permanent region of the HF). To obtain the gene expression profile of the individual MSCs, we developed the following

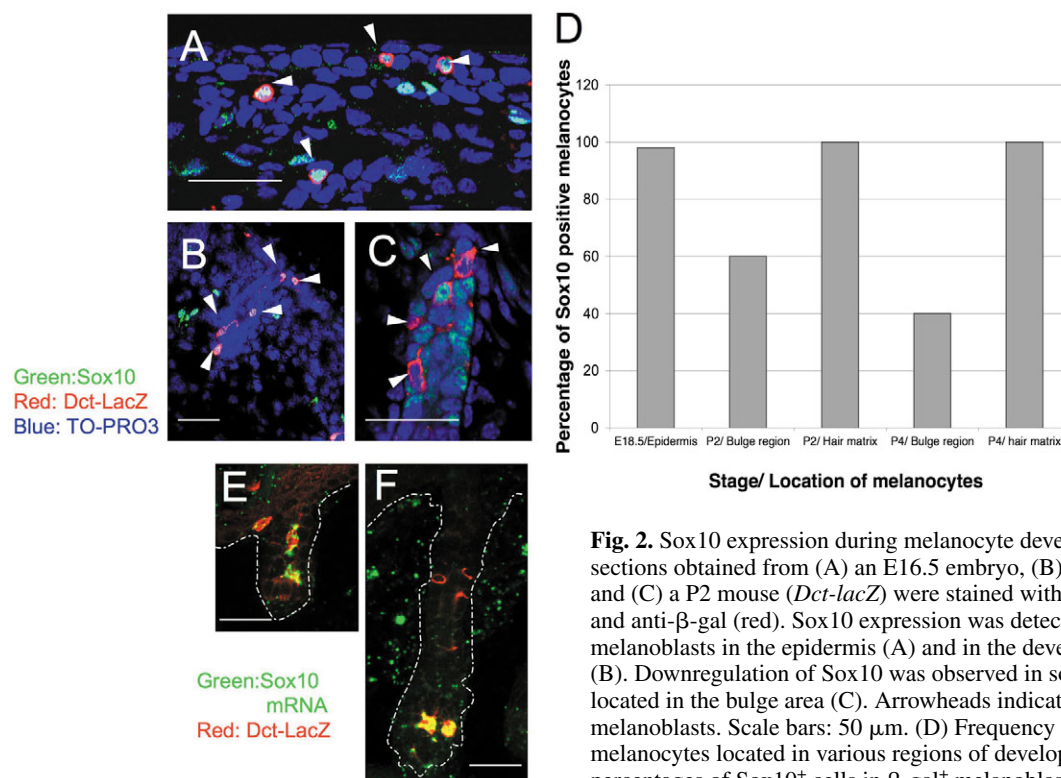


**Fig. 2.** Sox10 expression during melanocyte development. Skin sections obtained from (A) an E16.5 embryo, (B) an E18.5 embryo and (C) a P2 mouse (*Dct-lacZ*) were stained with anti-Sox10 (green) and anti-β-gal (red). Sox10 expression was detected in all β-gal<sup>+</sup> melanoblasts in the epidermis (A) and in the developing hair follicle (B). Downregulation of Sox10 was observed in some melanocytes located in the bulge area (C). Arrowheads indicate β-gal<sup>+</sup> melanoblasts. Scale bars: 50 μm. (D) Frequency of Sox10<sup>+</sup> melanocytes located in various regions of developing skin, shown as percentages of Sox10<sup>+</sup> cells in β-gal<sup>+</sup> melanoblasts located in the epidermis of the E18.5 embryo, or the bulge/sub-bulge region or hair matrix region of the P2 or P4 mice. Expression of *Sox10* mRNA was examined by in situ hybridization/immunohistochemistry double staining. (E) β-gal<sup>+</sup> (red) melanoblasts in a developing P2 hair follicle. All melanoblasts expressed *Sox10* mRNA (green). (F) Melanocytes in a P4 hair follicle. Some *Sox10*-negative melanocytes were observed in the bulge region. Scale bars: 50 μm.

matrix region of the P2 or P4 mice. (E,F) Downregulation of *Sox10* mRNA in bulge melanocytes. Expression of *Sox10* mRNA was examined by in situ hybridization/immunohistochemistry double staining. (E) β-gal<sup>+</sup> (red) melanoblasts in a developing P2 hair follicle. All melanoblasts expressed *Sox10* mRNA (green). (F) Melanocytes in a P4 hair follicle. Some *Sox10*-negative melanocytes were observed in the bulge region. Scale bars: 50 μm.

procedure to isolate single MCs from specific regions of the HF.

First, by combining enzymatic digestion of the dermis and the subcutaneous layer, and micro-dissection of stage 8 guard hairs from the epidermis, we established the conditions for harvesting the single HFs from the skin. As shown in Fig. 3A, the single HF isolated from a *Dct-lacZ* transgenic mouse was confirmed to contain some β-gal-positive MSCs in the bulge region, indicating the condition did not alter the existence of MSCs in the HF.

Next, to mark all the MCs in the epidermis, we engineered transgenic mice to express GFP in a MC-specific manner, by crossing *Dct/Cre* knock-in mice (*Dct<sup>tm1(Cre)Bee</sup>*) (Guyonneau et al., 2004) with *CAG-CAT-EGFP* reporter mice (Kawamoto et al., 2000) that express *GFP* under the control of a strong ubiquitous promoter, *CAG*, after the Cre-mediated removal of a Floxed *chloramphenicol acetyl transferase* (*CAT*) gene cassette (Fig. 3B). MC-specific GFP expression was confirmed in a single HF (Fig. 3C) and in embryonic epidermis (Fig. 3D) obtained from the transgenic mice. FACS analysis using embryonic epidermal cells revealed that the Cre-mediated recombination efficiency in the transgenic mice was more than 50%, as judged from the frequency of GFP<sup>+</sup> cells in the CD45<sup>-</sup>, Kit<sup>+</sup> Mbs (Fig. 3E).

To isolate individual MCs, single guard hairs of stage 8 HF morphogenesis were prepared from either Ack2-treated mice or non-treated mice. We regarded MSCs as the MCs remaining at the lower permanent portion of the HF in Ack2-treated mice,

and TA/DCs as the MCs localizing at the hair matrix in non-treated mice. The single HFs were further micro-dissected into the lower permanent portion and the hair matrix region under stereomicroscopy. After dissociation of each region into single cells by trypsin-EDTA treatment, individual GFP<sup>+</sup> cells were picked from the single-cell suspension under fluorescent microscopy. For comparison, single Mbs obtained from E16.5 embryonic epidermis were also picked. These cells were seeded into lysis buffer-containing PCR tubes and processed for gene expression analysis as described in the next section.

### Validation of the single-cell-based gene expression profiling technique

In order to perform high-throughput gene expression analysis from a limited amount of cells, a single-cell-based gene profiling strategy for the individual MCs was designed by combining single-cell cDNA amplification and a real-time PCR quantification assay (Q-PCR). We optimized and modified previous cDNA amplification methods (Iscove et al., 2002) to profile gene expression patterns by Q-PCR. Particularly, we modified the reverse transcription and PCR amplification steps to obtain the conditions that allowed the preservation of the initial representation of transcripts in Q-PCR assays, by maximizing the efficiency in the reverse transcription and minimizing the bias in amplification of transcripts during the cDNA amplification (see Materials and methods).

A crucial issue for the validation of our amplification

technique was to determine whether the relative expression value of each transcript in the amplified cDNA is representative of that of the original single-cell transcript in a reproducible fashion. To test the fidelity of cDNA amplification, we estimated the relative gene expression levels of individual genes in the amplified cDNA and examined how these correlated with the corresponding values obtained from unamplified cDNA. For this purpose, total RNA was prepared from a clonal Mb cell line, Melb-a (Sviderskaya et al., 1995), and cDNA was constructed either by conventional (unamplified) reverse transcription from 100 ng of the total RNA, or by performing PCR amplification with 10 pg of the total RNA, which is thought to be equivalent to half of that in a single cell. Relative gene expression values of 11 individual melanogenic genes were determined by Q-PCR using specific primers. Although there was a tendency for a distortion of the abundance relationships in some lower abundance transcripts, the estimated expression values of target genes in the amplified cDNA were roughly comparable to those in the unamplified cDNA (Fig. 4A). As shown in Fig. 4B, a significant correlation in the relative expression value of these 11 genes was observed between amplified and unamplified cDNA, indicating that the abundance relationships are relatively preserved by our cDNA amplification protocol. Thus, consistent with previous reports

(Iscove et al., 2002; Makrigiorgos et al., 2002), it is clear that our strategy preserved the abundance relationships by allowing semi-quantitative gene profiling, even at the single-cell level.

The second validation of cDNA amplification was to determine the reproducibility of our assay. To assess the reproducibility of cDNA amplification, we mixed in four distinct poly(A)-tailed *Arabidopsis thaliana* RNA spikes, each diluted to a known concentration (from 40 to  $4 \times 10^4$  copies), with 10 pg total RNA prepared from Melb-a cells, and amplified cDNA by cDNA amplification. We performed four replicate amplifications using aliquots of the same total RNA. Relative gene expression values were estimated by Q-PCR using a set of primer pairs specific for melanogenic genes, including *Actb*, *Dct*, *Mitf*, *Sox10*, *Tyrp1* and *Tyr*. As shown in Fig. 4C, the estimated expression value of each gene in amplified cDNA was very stable among four replicates, indicating the reproducibility of cDNA amplification. These validations clearly demonstrate that our cDNA amplification procedure is highly accurate and reproducible, and, thus, is suitable to be employed for single-cell transcript analysis.

To assess the sensitivity of our single-cell transcript analysis, we mixed various amounts of the four distinct RNA spikes into a constant amount (10 pg) of the total RNA and amplified cDNA by PCR amplification. As shown in Fig. 4D, subsequent Q-PCR analysis using the primers specific for each spike mRNA indicated that the abundance relationships were preserved between the Q-PCR quantification and the input copy number of each spike mRNA, allowing quantification assessment of mRNA copy numbers ranging from  $\sim 40$  to  $4 \times 10^5$ .

These data illustrate the ability of our cDNA amplification and Q-PCR quantification techniques to preserve the respective ratios of transcripts between the original RNA in a single cell and the amplified cDNA. Moreover, they demonstrate the capability of our single-cell transcript analysis system to detect low abundance transcripts; for example, less than 40 copies of mRNA.

### Single-cell transcriptional analysis of MSCs

Using this cDNA amplification method, we prepared cDNA from three different subsets of MCs, as described in previous section, and investigated the gene expression profiles in each subset. We also included four different concentrations of mRNA spikes (from 40 to  $4 \times 10^4$  copies) in the reaction mixture to ensure that the abundance relationships were preserved in each cDNA amplification. To avoid possible differences in the expression of the housekeeping genes that are normally used as internal standards for relative quantification in Q-PCR assay, we normalized the expression value of each gene to one of the mRNA spikes in order to perform accurate relative quantification by Q-PCR. cDNA was further evaluated to eliminate those failing to display significant expression of housekeeping genes such as *Gapd* and *Actb*, and/or failing to preserve the abundance relationships. In total, cDNA generated from 27/32 MSCs, 14/16 matrix MCs and 19/24 Mbs underwent gene profiling by Q-PCR using specific primer pairs (Fig. 5).

Various melanosome-organizing genes, including *Si*, *Tyrp1*, *Tyr*, *Mlana* and *Oa1* were downregulated in

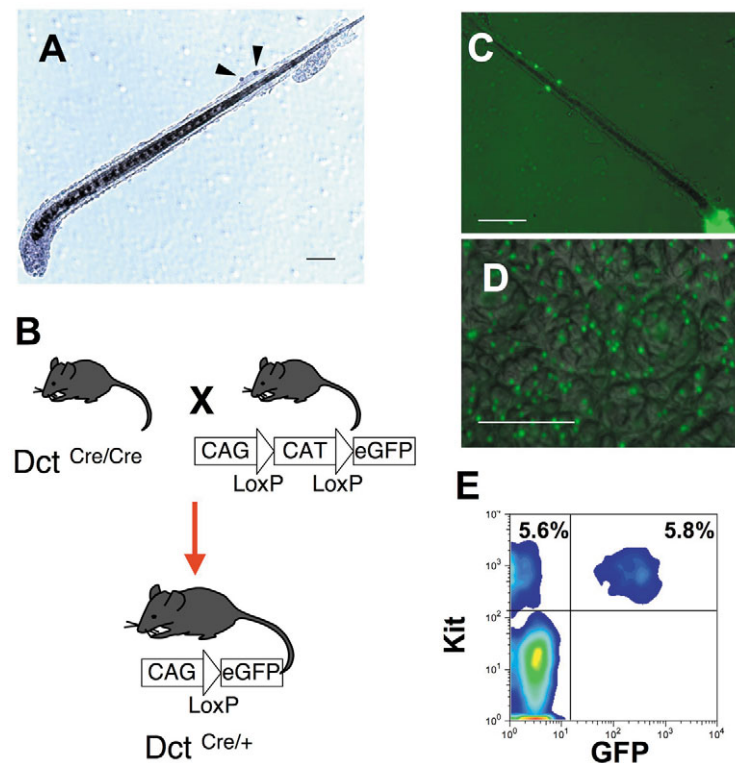


**Fig. 3.** System for in vivo labeling of the cells in the melanocyte lineage with GFP. Existence of MSCs in an isolated single hair follicle. Arrowheads indicate that MSCs reside in the lower permanent portion of the hair follicle. (B) Strategy for marking melanocytes with GFP. (C,D) GFP expression in a hair follicle and the embryonic epidermis. (E) FACS analysis of a single-cell suspension obtained from the epidermis of a melanocyte-specific GFP transgenic mouse at E16.5. The single-cell suspension was stained with PE-anti-CD45 and APC-anti-c-Kit, and processed for FACS analysis. The FACS profile of the cells in CD45-negative population is shown. Scale bars: 50  $\mu$ m.

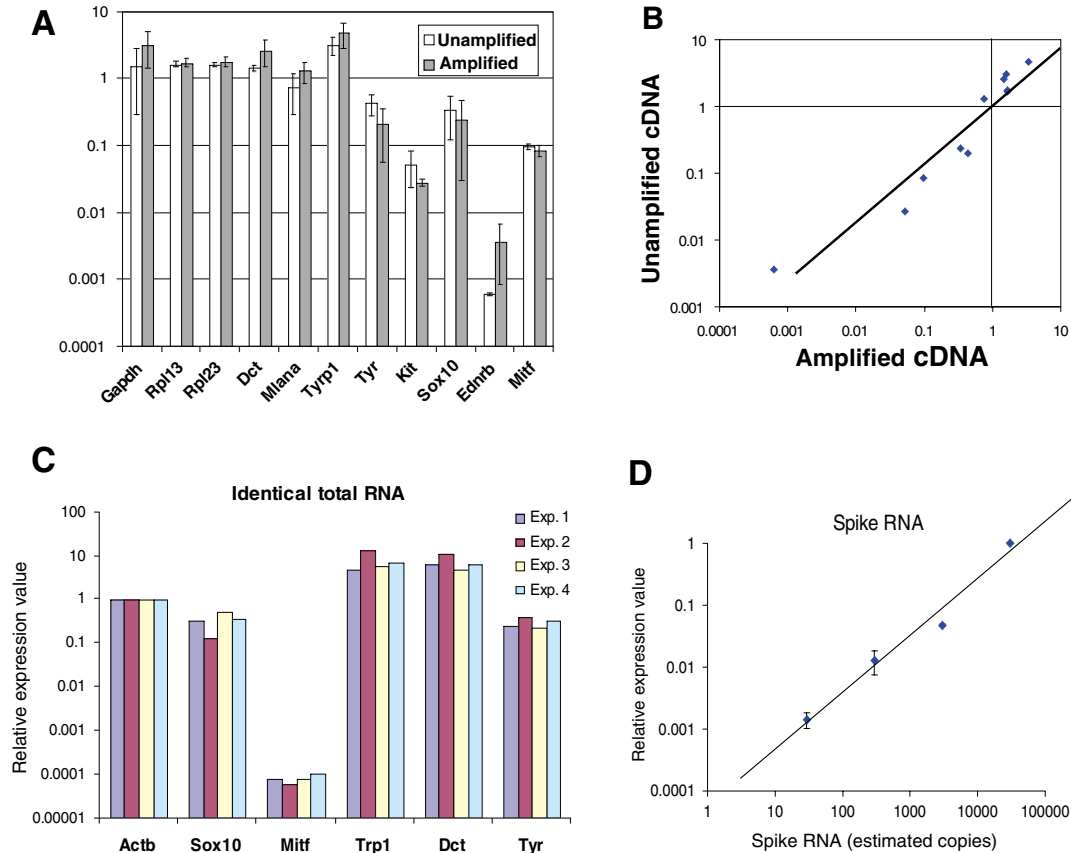


**Fig. 4.** Quantitative comparison of amplified cDNA with unamplified cDNA. (A) The relative gene expression level of each target gene in amplified cDNA (gray column) was compared with that in unamplified cDNA (white column). Data represent the average of three experiments. Error bars indicate s.d. (B) Scatter plot showing the relationship between relative gene expression values obtained from amplified and unamplified cDNA. Data obtained from Fig. 3B were plotted. (C) Reproducibility of cDNA amplification. Expression values of the melanogenic genes were determined by Q-PCR using four replicates of amplified cDNA. The expression value of each gene was consistent among the four amplifications. (D) Detection of transcripts at known copy number in cDNA amplification. Control poly(A)-tailed RNAs of known concentrations were mixed in lysis buffer containing 20 pg total RNA prepared from Melb-a cells, reverse transcribed followed by cDNA amplification. Four different RNA spikes, corresponding roughly to 40, 400, 4000 and 40,000 copies/sample, were spiked into four different tubes containing an identical amount of total RNA. Relative expression values were determined by Q-PCR using a primer pair specific for each spike RNA.

MSCs; however, their extensive expression was observed in the matrix MCs, reflecting the active melanin synthesis in matrix MCs. By contrast, the expression of these melanosome genes fluctuated in Mbs, suggesting that, in terms of melanosome maturation, Mbs are heterogeneous. *Si*, which is one of the earliest markers for melanosome maturation, was expressed in both Mbs and the matrix MCs. Consistent with immunohistochemical staining, quite a few MSCs express a low level of *Si* (3/27). Expression of cell surface receptors, including *Kit* and *Ednr*, was dramatically downregulated in the MSC population, whereas their expression was detected in the majority of Mbs (17/19 and 15/19, respectively) and in all of the matrix MCs. *Mclr* was predominantly expressed in the matrix MCs, although its expression was detected in a few of the Mbs and MSCs (1/19 and 2/27, respectively). As would be expected from the immunostaining (Fig. 1) and in situ hybridization analysis (Fig. 2A-F), *Sox10* expression was dramatically reduced in the MSC population (a low level of the expression was detected in 6/27), whereas extensive expression of *Sox10* was observed in Mbs (17/19) and in all of the matrix

MCs. Expression of *Mitf* was detected in many MCs throughout all of the subsets; however, its expression fluctuated greatly in these subsets.

In addition to the downregulation of the melanogenic genes in MSCs, the expression of some housekeeping genes (e.g. *Aldoa*) was found to be several orders of magnitude lower in MSCs than in TA cells/DCs or in Mbs.

## Discussion

### Isolation of single MSCs

In these studies, we exemplify one strategy for the isolation and molecular characterization of SCs. Except for HSCs, which can be isolated by a series of specific cell-surface markers (Arai et al., 2004), the isolation of SCs from many other SC systems has been complicated by their extreme rareness and the absence of specific markers. One possible way to identify SCs is to label the infrequently cycling LRCs through BrdU nuclear labeling experiments, although the identification of LRCs requires cell fixation, which may

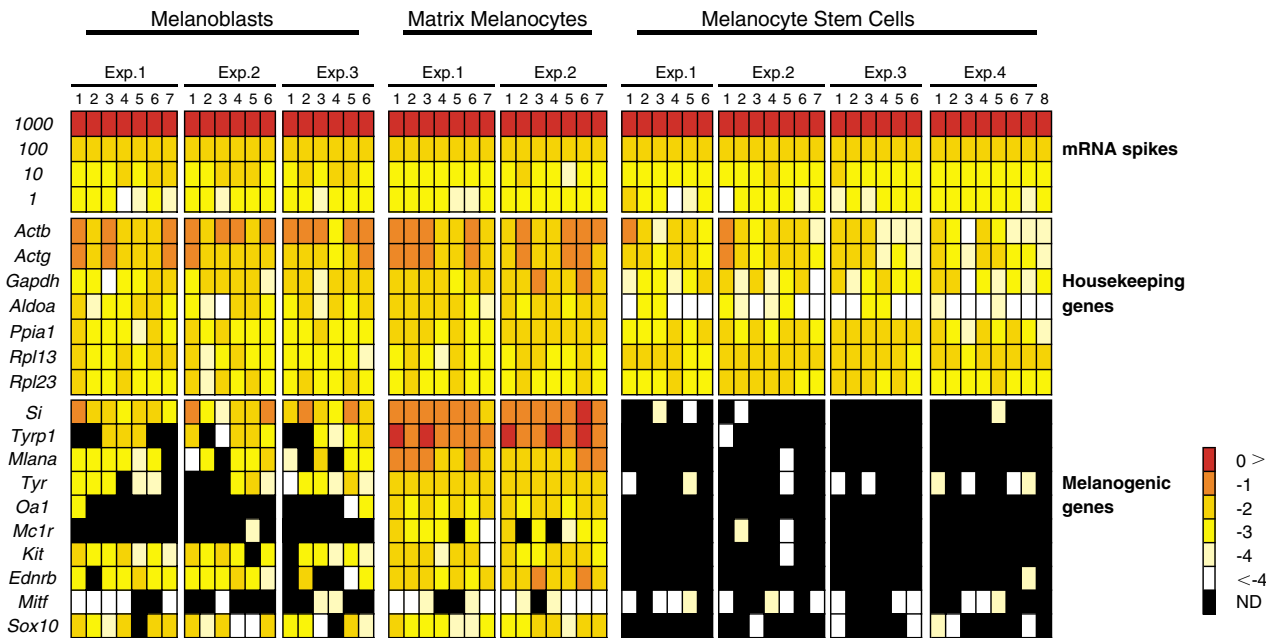


**Fig. 5.** Gene expression profiles of MSCs, TA cells/DCs and Mbs. The expression profiles of various genes in individual MSCs from the lower permanent portion of the hair follicle, and in hair matrix melanocytes (TA/DCs) and Mbs from the E16.5 epidermis are shown. The relative expression values for each gene were normalized against one of the mRNA spikes. To display gene expression profiles graphically, each relative expression value was transformed to a logarithmic value. Cells with a value of higher than 0 were classified as red, between 0 and -1 as orange, between -1 and -2 as light orange, between -2 and -3 as yellow, between -3 and -4 as pale yellow, and lower than -4 as white. Black shows that gene expression was not detected.

hamper high-quality gene expression analysis. Recently, this situation has been greatly improved by the development of a method to isolate LRCs that retain GFP-tagged histone 2B (H2B-GFP) for long time periods after the transient expression of H2B-GFP at certain times in development (Tumbar et al., 2004), although it is still unclear whether all LRCs are SCs.

Here, by using transgenic mice in which MCs are labeled with GFP following MC-specific Cre/LoxP recombination, we describe a method for the isolation of MSCs from the HF. Taking account of our previous observations (Nishimura et al., 2002), we regarded the GFP<sup>+</sup> cells that remain in the lower permanent portion of the HF after Ack2 treatment as quiescent MSCs. Cells in the TA/DC compartment are also identifiable at the hair matrix region in the non-treated HF. Because morphogenesis of the hair follicle is not synchronous, in order to avoid possible fluctuations in gene expression in MSCs at different hair follicle stages, we analyzed the gene expression profile of Ack2-resistant MSCs that resided in stage 8 guard hairs. We optimized the conditions for isolating individual MCs from the bulge/sub-bulge or hair matrix regions of single HFs, and single GFP<sup>+</sup> MSCs, TA cells/DCs or Mbs were picked.

We believe that this strategy for the isolation of SCs has the following advantages over other possible cell separation techniques, such as FACS. First, it should be the most accurate and precise way to isolate SCs, if SCs are anatomically or morphologically identifiable. The strategy is expected to be applicable for the isolation of SCs, such as spermatogonial SCs, muscle satellite cells or SCs for the intestinal epithelium, whose location has been well defined. Second, it is expected

to be advantageous for the isolation of niche-forming cells, which are thought to be closely associated with SCs. The niche-forming cells for GSCs in the *Drosophila* ovary (Xie and Spradling, 2000) and for HSCs in murine bone marrow (Calvi et al., 2003; Zhang et al., 2003) have been already demonstrated. However, except for these few examples, niche cells are still conceptual for most SCs. Under such circumstances, the only way to harvest niche-forming cells, if they exist, is to collect cells located around the SCs. Gene profiling of the cells that surround the GFP<sup>+</sup> MSCs is currently under way in our laboratory.

### Single-cell-based gene expression analysis

In this study, we applied cDNA amplification to obtain gene expression profiles for individual MSCs. We adopted single-cell-derived cDNA amplification for Q-PCR assay, which allowed the simple and high-throughput quantification of gene expression at single-cell level. The validation of our cDNA amplification demonstrated that this procedure is reproducible, faithfully represents the gene expression profile of a single cell, and maintains the abundance relationships of transcripts, ranging from ~40 to 4×10<sup>5</sup> copies in an individual cell.

Unlike microarray analysis, which allows the expression of ~30,000 genes to be profiled at a time, this technique is suitable for analyzing the gene expression of ~100 individual genes simultaneously. Because the number of PCR cycles in the cDNA amplification step is restricted to 25, the total yield of cDNA in our amplification is less than ~50 ng, which is several orders of magnitude less than the amount required for microarray hybridization. We tried to increase the number of amplification cycles to obtain more cDNA; however, this

resulted in distortion of the abundance relationships of spike mRNAs in the Q-PCR analysis.

Like all gene expression analysis methods, the strategy described here has limitations. Because our single-cell cDNAs represent ~600 bp from the 3' ends of the transcripts, the primer set should be designed within this range to obtain a PCR product. However, despite the massive effort to define entire genome sequences, the information on 3'-end transcripts in the databases is still poor. This limitation is sometimes critical for our strategy. Indeed, we never detected a Pax3 transcript, in any of our MC subsets, with any of the primer pairs that were designed to be specific for the 3'-end region of Pax3 using information from the Ensembl Mouse Genome Database, although all of the primer pairs worked nicely with conventional RT-PCR. One possible explanation for this might be that the Pax3 3'-end information in the database is incomplete.

Another possible limitation of single-cell profiling stems from the fact that, in clonal population, cells can exhibit substantial phenotypic variation, particularly in the expression of low copy number molecules. It has been reported that both intrinsic and extrinsic noise affects gene expression in a stochastic manner (Elowitz et al., 2002; McAdams and Arkin, 1997). In addition to this stochasticity in transcription, recent studies have revealed that the levels of cellular mRNA transcripts are temporally regulated by active mRNA decay (Wilusz et al., 2001). The regulation of mRNA decay is critically important to determine the abundance of cellular transcripts. As shown in the previous report (Herrick et al., 1990), decay rates of individual mRNA transcripts differ extensively; some vital mRNAs are degraded rapidly by certain destabilizing protein complexes or by RNA interference machinery, whereas other mRNAs are maintained for several generations. As a consequence of these combinatory regulations, mRNA transcripts in individual cells could vary dynamically over time. These differences in gene expression may account for the cell-cell variation observed in clonal populations, and are thought to play crucial roles in fundamental biological processes (Heitzler and Simpson, 1991). These variations are not evident when gene expression profiling is performed at the population level; however, they are critical for single-cell based analysis. In this study, we noticed fluctuations in the expression of several genes, such as *Mitf*. Consistent with our data, several other reports (Chiang and Melton, 2003; Peixoto et al., 2004; Saitou et al., 2002; Theilgaard-Monch et al., 2001; Tietjen et al., 2003) also showed considerable cell-to-cell variations in their single-cell transcript analysis. Taken together with these single-cell transcript analyses, our data clearly indicate that mRNA transcripts in individual cells intrinsically fluctuate, which may require a new paradigm of transcript analysis to understand its biological significance.

In addition to these cell-autonomous fluctuations, variations in gene expression in MSCs may arise from the differences in hair cycles or hair types in which the MSCs are localized. Because hair follicle morphogenesis follows a rather precise time-scale, we focused our analysis on the MCs localized in guard hairs at stage 8 of hair follicle morphogenesis to standardize the stage and the type of HF. However, we could not exclude the possibility that gene expression is affected by the difference in the precise location of MSCs in the niche, as

it has been demonstrated that several different types of epidermal SCs are localized at different positions within the bulge region (Blanpain et al., 2004).

In these circumstances, the key issue for single-cell transcript analysis is to distinguish the biologically significant transcriptional differences from the intrinsic fluctuations in the mRNA copy number in single cells. We therefore performed multiple gene expression profiling using 62 single cells, ensuring the gene expression profile by immunohistochemical staining or in situ staining. We could not detect the expression of some crucial genes for melanogenesis, including *Sox10* and *Kit*, in the stem cell population reproducibly, which was consistent with the immunostaining results. Thus the data convincingly demonstrates that the gene expression profile of the melanocyte stem cells is significantly different from the intrinsic fluctuations observed in gene expression in other populations, although we cannot completely exclude the possibility that random inaccuracies in the reverse transcription and cDNA amplification distort the real expression patterns in low abundance transcripts (less than 40 copies).

Besides these limitations, we expect this strategy to be advantageous over microarray analysis for obtaining a quick sketch of the gene expression profile in a given cell species; microarray analysis may deliver comprehensive gene expression data, but it requires multiple samples to obtain reproducible data and complicated statistical analysis. In particular, our strategy allows us to understand the diversity of individual cells on a transcriptional basis among a given population located in a restricted area, such as the SC niche.

### Signature of MSCs

To confirm that MSCs were harvested properly, it was necessary to distinguish the SC compartment from other compartments. For this purpose, we stained HFs with antibodies against proteins whose roles have been implicated in MC development. We identified the following two groups of protein. The first group included *Dct* and *Pax3*, whose expression was observed both in MSCs and in TA cells/DCs. The second group of molecules was highly expressed only in the TA cells/DCs, and included *Kit*, *Si*, *Tyr*, *Tyrp1*, *Mki67*, *Lef1*, *Sox10* and *Mitf*. We could not specify molecules expressed only in MSCs. Nevertheless, we used this expression pattern as a signature for distinguishing MSCs from cells from other compartments, and examined whether this pattern was consistent with that in each available single-cell cDNA.

As shown in Fig. 5, the SC signature defined by immunohistochemistry (Fig. 1) was basically represented in the gene expression profiles of MSCs (Fig. 5), although some discrepancies were observed. For instance, low levels of *Si* and *Tyrp1* transcripts were detected in few MSCs even though protein expression was not detected in the SCs. These discrepancies might be explained by the level of these proteins being below the detection limit of our immunostaining, or by the existence of post-transcriptional regulation in the SCs, as has been reported in various SCs and progenitors.

While defining the signature of the SCs, we observed that *Sox10* expression was far lower in the SCs than in the TA cells/DCs. This observation was confirmed by both in situ hybridization and gene expression profiling. Decreased *Sox10* expression in the SCs could be due to repression or to a lack of activation of its transcription. Moreover, our analysis of

*Sox10* expression during development of the HF strongly suggests that *Sox10* is actively downregulated upon Mb colonization of the lower permanent region. This is consistent with our previous study showing that the MSC niche plays a dominant role in directing MC fate (Nishimura et al., 2002). Although further studies are needed to understand the significance of this observation, we expect the repression of *Sox10* transcription in the MSCs to provide an important clue for understanding the mechanism underlying the maintenance of resting SCs by the niche.

### Regulation of SCs by the niche

We demonstrated the molecular expression profile of MSCs in the niche. Here, by combining immunostaining and gene expression profiling, we have observed the downregulation of various key melanogenic factors and genes, including *Sox10*, *Mitf*, *Kit*, *Lef1* and *Ednrb*, indicating that MSCs utilize a different biochemistry from that of TA cells/DCs to maintain their physiological features. Interestingly, our gene expression analysis also shows the downregulation of some housekeeping genes in MSCs (Fig. 5). Taken together with the relative quiescence of MSCs (Nishimura et al., 2002), these data support the idea that basal transcription is downregulated in the SC population, as it is characterized that cellular quiescence is a state accompanied by lower rates of transcription, translation and metabolism (Yusuf and Fruman, 2003). Thus, these data clearly suggest a role for the niche in regulating molecular expression in MSCs, both at the transcriptional and translational level. In MCs, molecular interactions among these key melanogenic molecules have been well documented (Goding, 2000; Lin and Spradling, 1997; McGill et al., 2002; Saito et al., 2002; Takeda et al., 2000), and it is obvious that their downregulation in the SC compartment blocks the growth and/or differentiation cues in MCs. Taken together with recent genetic studies of epidermal SCs (Blanpain et al., 2004; Morris et al., 2004; Tumber et al., 2004), we propose that one of the key strategies of SC regulation by the niche is to insulate SCs from various activation stimuli that promote growth and/or differentiation cues in the SC compartment, by downregulating their receptors or key signaling mediators, and/or by inducing inhibitory factors against the activating stimuli.

We thank Drs Y. Yabuta, K. Kurimoto and M. Saitou (RIKEN CDB, Japan) for technical advice on the quantitative amplification of single-cell cDNA. We are grateful to the Laboratory for Animal Resources and Genetic Engineering in RIKEN CDB for generation of the transgenic mice and for the housing of animals. We also thank Dr J. Miyazaki for *CAG-CAT-GFP* mice, Dr I. Jackson for *Dct-lacZ* mice, Dr H. Yamamoto for the anti-Mitf antibody, Dr V. Hearing for the anti-Dct, Tyrp1 and Si antibodies, Dr M. Wegner for the *Sox10* antibody and cDNA, and Dr G. Grosveld for the anti-Pax3 antibody. This work was supported in part by Grant-in-Aid for Scientific Research on Priority Areas (12219209 to S.-I.N. and 15039236 to M.O.) and by a grant for Regenerative Medicine Realization Projects from the Ministry of Education, Culture, Sports, Science and Technology of Japan.

### References

Arai, F., Hirao, A., Ohmura, M., Sato, H., Matsuoka, S., Takubo, K., Ito, K., Koh, G. Y. and Suda, T. (2004). Tie2/angiopoietin-1 signaling regulates hematopoietic stem cell quiescence in the bone marrow niche. *Cell* **118**, 149-161.

Blanpain, C., Lowry, W. E., Geoghegan, A., Polak, L. and Fuchs, E. (2004). Self-renewal, multipotency, and the existence of two cell populations within an epithelial stem cell niche. *Cell* **118**, 635-648.

Bondurand, N., Pingault, V., Goerich, D. E., Lemort, N., Sock, E., Caignec, C. L., Wegner, M. and Goossens, M. (2000). Interaction among *SOX10*, *PAX3* and *MITF*, three genes altered in Waardenburg syndrome. *Hum. Mol. Genet.* **9**, 1907-1917.

Botchkareva, N. V., Khlgatian, M., Longley, B. J., Botchkarev, V. A. and Gilchrist, B. A. (2001). SCF/c-kit signaling is required for cyclic regeneration of the hair pigmentation unit. *FASEB J.* **15**, 645-658.

Calvi, L. M., Adams, G. B., Weibrecht, K. W., Weber, J. M., Olson, D. P., Knight, M. C., Martin, R. P., Schipani, E., Divieti, P., Bringham, F. R. et al. (2003). Osteoblastic cells regulate the haematopoietic stem cell niche. *Nature* **425**, 841-846.

Cheng, T., Rodrigues, N., Shen, H., Yang, Y., Dombkowski, D., Sykes, M. and Scadden, D. T. (2000). Hematopoietic stem cell quiescence maintained by p21cip1/waf1. *Science* **287**, 1804-1808.

Cheshier, S. H., Morrison, S. J., Liao, X. and Weissman, I. L. (1999). In vivo proliferation and cell cycle kinetics of long-term self-renewing hematopoietic stem cells. *Proc. Natl. Acad. Sci. USA* **96**, 3120-3125.

Chiang, M. K. and Melton, D. A. (2003). Single-cell transcript analysis of pancreas development. *Dev. Cell* **4**, 383-393.

Cotsarelis, G., Sun, T. T. and Lavker, R. M. (1990). Label-retaining cells reside in the bulge area of pilosebaceous unit: implications for follicular stem cells, hair cycle, and skin carcinogenesis. *Cell* **61**, 1329-1337.

Elowitz, M. B., Levine, A. J., Siggia, E. D. and Swain, P. S. (2002). Stochastic gene expression in a single cell. *Science* **297**, 1183-1186.

Fuchs, E., Tumber, T. and Guasch, G. (2004). Socializing with the neighbors: stem cells and their niche. *Cell* **116**, 769-778.

Goding, C. R. (2000). Mitf from neural crest to melanoma: signal transduction and transcription in the melanocyte lineage. *Genes Dev.* **14**, 1712-1728.

Groszer, M., Erickson, R., Scripture-Adams, D. D., Lesche, R., Trumpp, A., Zack, J. A., Kornblum, H. I., Liu, X. and Wu, H. (2001). Negative regulation of neural stem/progenitor cell proliferation by the Pten tumor suppressor gene in vivo. *Science* **294**, 2186-2189.

Guyonneau, L., Murisier, F., Rossier, A., Moulin, A. and Beermann, F. (2004). Melanocytes and pigmentation are affected in dopachrome tautomerase knockout mice. *Mol. Cell. Biol.* **24**, 3396-3403.

Heitzler, P. and Simpson, P. (1991). The choice of cell fate in the epidermis of *Drosophila*. *Cell* **64**, 1083-1092.

Herrick, D., Parker, R. and Jacobson, A. (1990). Identification and comparison of stable and unstable mRNAs in *Saccharomyces cerevisiae*. *Mol. Cell. Biol.* **10**, 2269-2284.

Iscove, N. N., Barbara, M., Gu, M., Gibson, M., Modi, C. and Winegarden, N. (2002). Representation is faithfully preserved in cDNA amplified exponentially from sub-picogram quantities of mRNA. *Nat. Biotechnol.* **20**, 940-943.

Jordan, S. A. and Jackson, I. J. (2000). A late wave of melanoblast differentiation and rostrocaudal migration revealed in patch and rump-white embryos. *Mech. Dev.* **92**, 135-143.

Kawamoto, S., Niwa, H., Tashiro, F., Sano, S., Kondoh, G., Takeda, J., Tabayashi, K. and Miyazaki, J. (2000). A novel reporter mouse strain that expresses enhanced green fluorescent protein upon Cre-mediated recombination. *FEBS Lett.* **470**, 263-268.

Kiger, A. A., Jones, D. L., Schulz, C., Rogers, M. B. and Fuller, M. T. (2001). Stem cell self-renewal specified by JAK-STAT activation in response to a support cell cue. *Science* **294**, 2542-2545.

Lin, H. and Spradling, A. C. (1997). A novel group of pumilio mutations affects the asymmetric division of germline stem cells in the *Drosophila* ovary. *Development* **124**, 2463-2476.

Mackenzie, M. A., Jordan, S. A., Budd, P. S. and Jackson, I. J. (1997). Activation of the receptor tyrosine kinase Kit is required for the proliferation of melanoblasts in the mouse embryo. *Dev. Biol.* **192**, 99-107.

Mahmud, N., Devine, S. M., Weller, K. P., Parmar, S., Sturgeon, C., Nelson, M. C., Hewett, T. and Hoffman, R. (2001). The relative quiescence of hematopoietic stem cells in nonhuman primates. *Blood* **97**, 3061-3068.

Makrigiorgos, G. M., Chakrabarti, S., Zhang, Y., Kaur, M. and Price, B. D. (2002). A PCR-based amplification method retaining the quantitative difference between two complex genomes. *Nat. Biotechnol.* **20**, 936-939.

McAdams, H. H. and Arkin, A. (1997). Stochastic mechanisms in gene expression. *PNAS* **94**, 814-819.

McGill, G. G., Horstmann, M., Widlund, H. R., Du, J., Motyckova, G., Nishimura, E. K., Lin, Y. L., Ramaswamy, S., Avery, W., Ding, H. F. et

- al. (2002). Bcl2 regulation by the melanocyte master regulator Mitf modulates lineage survival and melanoma cell viability. *Cell* **109**, 707-718.
- Mollaaghababa, R. and Pavan, W. J.** (2003). The importance of having your SOX on: role of SOX10 in the development of neural crest-derived melanocytes and glia. *Oncogene* **22**, 3024-3034.
- Morris, R. J., Liu, Y., Marles, L., Yang, Z., Trempus, C., Li, S., Lin, J. S., Sawicki, J. A. and Cotsarelis, G.** (2004). Capturing and profiling adult hair follicle stem cells. *Nat. Biotechnol.* **22**, 411-417.
- Nakamura, M., Tobin, D. J., Richards-Smith, B., Sundberg, J. P. and Paus, R.** (2002). Mutant laboratory mice with abnormalities in pigmentation: annotated tables. *J. Dermatol. Sci.* **28**, 1-33.
- Nishikawa, S., Kusakabe, M., Yoshinaga, K., Ogawa, M., Hayashi, S., Kunisada, T., Era, T., Sakakura, T. and Nishikawa, S.** (1991). In utero manipulation of coat color formation by a monoclonal anti-c-kit antibody: two distinct waves of c-kit-dependency during melanocyte development. *EMBO J.* **10**, 2111-2118.
- Nishimura, E. K., Jordan, S. A., Oshima, H., Yoshida, H., Osawa, M., Moriyama, M., Jackson, I. J., Barrandon, Y., Miyachi, Y. and Nishikawa, S.** (2002). Dominant role of the niche in melanocyte stem-cell fate determination. *Nature* **416**, 854-860.
- Nishimura, E. K., Granter, S. R. and Fisher, D. E.** (2005). Mechanisms of hair graying: incomplete melanocyte stem cell maintenance in the niche. *Science* **307**, 720-724.
- Paus, R., Muller-Rover, S., Van Der Veen, C., Maurer, M., Eichmuller, S., Ling, G., Hofmann, U., Foitzik, K., Mecklenburg, L. and Handjiski, B.** (1999). A comprehensive guide for the recognition and classification of distinct stages of hair follicle morphogenesis. *J. Invest. Dermatol.* **113**, 523-532.
- Peixoto, A., Monteiro, M., Rocha, B. and Veiga-Fernandes, H.** (2004). Quantification of multiple gene expression in individual cells. *Genome Res.* **14**, 1938-1947.
- Potten, C. S. and Loeffler, M.** (1990). Stem cells: attributes, cycles, spirals, pitfalls and uncertainties. Lessons for and from the crypt. *Development* **110**, 1001-1020.
- Potterf, S. B., Mollaaghababa, R., Hou, L., Southard-Smith, E. M., Hornyak, T. J., Arnheiter, H. and Pavan, W. J.** (2001). Analysis of SOX10 function in neural crest-derived melanocyte development: SOX10-dependent transcriptional control of dopachrome tautomerase. *Dev. Biol.* **237**, 245-257.
- Saito, H., Yasumoto, K.-i., Takeda, K., Takahashi, K., Fukuzaki, A., Orikasa, S. and Shibahara, S.** (2002). Melanocyte-specific microphthalmia-associated transcription factor isoform activates its own gene promoter through physical interaction with lymphoid-enhancing factor 1. *J. Biol. Chem.* **277**, 28787-28794.
- Saitou, M., Barton, S. C. and Surani, M. A.** (2002). A molecular programme for the specification of germ cell fate in mice. *Nature* **418**, 293-300.
- Schofield, R.** (1978). The relationship between the spleen colony-forming cell and the haemopoietic stem cell. *Blood Cells* **4**, 7-25.
- Shin, M. K., Levorse, J. M., Ingram, R. S. and Tilghman, S. M.** (1999). The temporal requirement for endothelin receptor-B signalling during neural crest development. *Nature* **402**, 496-501.
- Spradling, A., Drummond-Barbosa, D. and Kai, T.** (2001). Stem cells find their niche. *Nature* **414**, 98-104.
- Sviderskaya, E. V., Wakeling, W. F. and Bennett, D. C.** (1995). A cloned, immortal line of murine melanoblasts inducible to differentiate to melanocytes. *Development* **121**, 1547-1557.
- Takeda, K., Yasumoto, K.-i., Takada, R., Takada, S., Watanabe, K.-i., Uono, T., Saito, H., Takahashi, K. and Shibahara, S.** (2000). Induction of melanocyte-specific microphthalmia-associated transcription factor by Wnt-3a. *J. Biol. Chem.* **275**, 14013-14016.
- Theilgaard-Monch, K., Cowland, J. and Borregaard, N.** (2001). Profiling of gene expression in individual hematopoietic cells by mRNA amplification and slot blot analysis. *J. Immunol. Methods* **252**, 175-189.
- Tietjen, I., Rihel, J. M., Cao, Y., Koentges, G., Zakhary, L. and Dulac, C.** (2003). Single-cell transcriptional analysis of neuronal progenitors. *Neuron* **38**, 161-175.
- Tulina, N. and Matunis, E.** (2001). Control of stem cell self-renewal in Drosophila spermatogenesis by JAK-STAT signaling. *Science* **294**, 2546-2549.
- Tumbar, T., Guasch, G., Greco, V., Blanpain, C., Lowry, W. E., Rendl, M. and Fuchs, E.** (2004). Defining the epithelial stem cell niche in skin. *Science* **303**, 359-363.
- Walkley, C. R., Fero, M. L., Chien, W. M., Purton, L. E. and McArthur, G. A.** (2005). Negative cell-cycle regulators cooperatively control self-

- renewal and differentiation of haematopoietic stem cells. *Nat. Cell. Biol.* **7**, 172-178.
- Watt, F. M. and Hogan, B. L.** (2000). Out of Eden: stem cells and their niches. *Science* **287**, 1427-1430.
- Wilkinson, D. G. and Nieto, M. A.** (1993). Detection of messenger RNA by in situ hybridization to tissue sections and whole mounts. *Methods Enzymol.* **225**, 361-373.
- Wilusz, C. J., Wormington, M. and Peltz, S. W.** (2001). The cap-to-tail guide to mRNA turnover. *Nat. Rev. Mol. Cell. Biol.* **2**, 237-246.
- Xie, T. and Spradling, A. C.** (2000). A niche maintaining germ line stem cells in the Drosophila ovary. *Science* **290**, 328-330.
- Yusuf, I. and Fruman, D. A.** (2003). Regulation of quiescence in lymphocytes. *Trends Immunol.* **24**, 380-386.
- Zhang, J., Niu, C., Ye, L., Huang, H., He, X., Tong, W. G., Ross, J., Haug, J., Johnson, T., Feng, J. Q. et al.** (2003). Identification of the haematopoietic stem cell niche and control of the niche size. *Nature* **425**, 836-841.